ELSEVIER

Journal of Alloys and Compounds 434–435 (2007) 550–554

Journal of ALLOYS AND COMPOUNDS

www.elsevier.com/locate/jallcom

Metropolis Monte Carlo predictions of free Co–Pt nanoclusters

P. Moskovkin [a,b], M. Hou [a,*]

[a] *Physique des Solides Irradiés et des Nanostructures CP234, Université Libre de Bruxelles, Bd du Triomphe, B-1050 Bruxelles, Belgium*
[b] *RRC "Kurchatov Institute", Moscow, Russia*

Available online 26 September 2006

Abstract

The Metropolis Monte Carlo (MC) sampling method with a semi-empirical Embedded Atom Model (EAM) and a Modified EAM (MEAM) potentials is used to investigate structural properties of free Co–Pt nanoclusters. Sampling is achieved in the number–pressure–temperature (NPT) and the ($\Delta\mu$-NPT) ensembles, where $\Delta\mu$ denotes the chemical potential difference between the Co and Pt subsystems. The model potentials are parameterised on the basis of the structure, the lattice distance, the vacancy formation energy, the bulk modulus and the cohesive energy of pure cobalt and platinum. The mixed repulsive contribution to the EAM configuration energy is here tuned in such a way to correctly predict the tetragonal ordered structure of CoPt at room temperature. MC predicts the ordered structure of Co_3Pt, CoPt and $CoPt_3$ phases as well as the order–disorder phase transition in CoPt. The results obtained with both potentials are compared. The study is then extended to isolated CoPt and Co_3Pt clusters containing a few hundred atoms and the consequences of temperature on predicted structural and segregation properties are investigated.

Keywords: Clusters; Intermetallics; Nanostructures; Metals; Surfaces; Interfaces

1. Introduction

The cobalt–platinum system is known for its interesting magnetic properties. CoPt multilayers display a perpendicular anisotropy which limits the dipolar coupling between magnetic domains and a high anisotropy which warrants the stability of these domains. It is now possible, using laser vaporization techniques [1] to produce clusters made of cobalt and platinum with any composition and of any size less than 10 nm, and to deposit them at supersonic velocities on a substrate. This allows the hope to tune and to optimise the particle properties at wealth and to design recording devices with a density in the Tbits/in.^{2} range. A first step in this direction is already achieved by trapping clusters on a nanopatterned surface [2].

Depending upon their composition, bulk Co–Pt alloys display structural phases where crystallography is related to their magnetic performances. This is the case for the $L1_0$ CoPt phase, made of alternate pure Co and pure Pt planes. As far as the nanoparticles are concerned, the surface to volume ratio is so high that surfaces may play a prominent role in the particle properties. Subsequently, these structural and magnetic properties may substantially differ from those of bulk materials. A systematic experimental study of the structural and magnetic properties of Co–Ag and Co–Pt nanoparticles has been recently started [3–5], which appeals for theoretical understanding. Since nanoparticles contain no more than a few thousand atoms, atomic scale modelling methods are ideally suited for their study. However, to our knowledge, none is yet available as far as the CoPt nanoparticles are concerned.

Structural properties of Co_3Pt, CoPt and $CoPt_3$ bulk alloys were already studied at the atomic scale in [6] by means of Metropolis Monte Carlo (MMC) importance sampling, with a special focus on order–disorder transitions. A realistic cohesion model was used; therefore, in the present study, a similar approach is used, based on a somewhat more general algorithm, with the purpose of emphasizing the role of the cohesion model on phase stability and the study is extended to Co–Pt nanoparticles.

In Section 2, the main characteristics of the Embedded Atom Model (EAM) and of the Modified EAM (MEAM) are given and the MC algorithm and its variants used are briefly described. Order parameters are defined for the $L1_0$ and the $L1_2$ structures. Section 3 is subdivided into two parts. The first is devoted to structural and thermodynamic properties of bulk CoPt alloys

* Corresponding author at: Physique des Solides Irradiés et des Nanostructures CP234, Université Libre de Bruxelles, Bd du Triomphe, B-1050 Bruxelles, Belgium. Tel.: +32 2 650 5735; fax: +32 2 650 5227.
E-mail addresses: pmoskovkin@nfi.kiae.ru (P. Moskovkin), mhou@ulb.ac.be (M. Hou).

0925-8388/$ – see front matter © 2006 Elsevier B.V. All rights reserved.
doi:10.1016/j.jallcom.2006.08.178

and solid solutions and the second is devoted to CoPt and Co_3Pt nanoparticles.

2. The model

2.1. The model potentials

The main parameter governing interatomic interactions in an atomic scale model is the potential. For metals, many body interactions are accounted for, for instance, in the Embedded Atom. Its isotropic form has been generalised in order to take possible s, p, d and f hybridizations into account, leading to the so-called Modified EAM model.

The EAM and MEAM models are presented in [7–11] and we only give a brief description here.

The same EAM potential function was applied to study of the Ag–Co system [12–15].

In both the models, the expression for total energy is given in the form

$$E_c = \sum_i \left[F(\rho_i) + 0.5 \sum_{j \neq i} \Phi(R_{ij}) \right] \quad (1)$$

In this equation, ρ_i is a background electron density at the site of atom i, $F(\rho_i)$ is the embedded function, R_{ij} is the distance between atoms i and j, and $\Phi(R_i)$ is the pair potential. The EAM potential ranges to the 1.59 lattice distances while the range of the MEAM is limited to first neighbours and the screening function first suggested in [15] was used for limiting further neighbour interactions. The essential difference between the EAM and the MEAM lies in the functional dependence of $F(\rho_i)$ on the relative atomic positions. While it is isotropic in the EAM [7,8], it contains angular terms in the MEAM whose expressions are given in [9]. Both are parameterised so as to match the equation of state of Rose et al. [16].

2.2. The Metropolis Monte Carlo model

The Metropolis MC method is widely used for studying the equilibrium properties of liquids and solids. The general algorithm is well described, e.g. in [17]. Here we use two versions of it. The first is the so-called "modified grand-canonical ensemble with transmutations" ($\Delta\mu$-NPT) [18]. In this approach, the total number of the particles ($N = N_{Co} + N_{Pt}$), temperature (T), pressure (P) and chemical potentials difference ($\Delta\mu = \mu_{Al} - \mu_{Ni}$) are fixed. The partial number of each kind of atom (N_{Co}, N_{Pt}) may be changed. This is realistic in case of the synthesis of particles at equilibrium in an environment where both species are available in unlimited quantities. When particles are synthesised far out of equilibrium conditions however, the number of atoms of each species may be governed by other constraints. In laser vaporization environment, for instance, where particles are synthesised at very high temperature and then quenched, their stoichiometry is often the same as that of the source. When this happens, segregation at the particle surface implies a depletion of the segregated species in the core, which is not expected in conditions where the particle grows at equilibrium. In order to model this, no transmutation is allowed and the MC sampling is performed in the canonical ensemble. The MC algorithm includes three types of trials:

(i) Random displacement of each atom of the model box from its current position. The magnitude of this displacement is dynamically adjusted in order to optimise convergence. This optimised convergence was empirically found for an acceptance rate of 0.4, which is obtained here with random displacements of the order of a few 10^{-6} nm. The decision of acceptance of a new configuration is based on the relation between probabilities according to the standard Metropolis method:

$$\frac{P_{new}}{P_{old}} = \exp\left\{ -\frac{\Delta U}{kT} \right\} \quad (2)$$

where kT is the Boltzmann factor and ΔU is the potential energy difference. If the ratio P_{new}/P_{old} is larger than unity, the new configuration is accepted anyway. Otherwise, it is accepted with the probability P_{new}/P_{old}.

(ii) Chemical identity of an atom selected at random is changed with relative probability:

$$\frac{P_{new}}{P_{old}} = \exp\left\{ -\frac{\Delta U - \Delta\mu}{kT} \right\} \quad (3)$$

This trial is only used for sampling in the semi-grand-canonical ensemble.

(iii) The site of this atom is exchanged with another one selected at random in the box. The decision of acceptance in this case is based on the relation (2). Such exchanges correspond to no physical evolution path of the system but they improve the convergence of the algorithm.

One set of these three trials applied on all atoms in the system is called a "macrostep". After all atoms in the box have undergone several macrosteps, the lattice parameter of one of the randomly selected box direction [0 0 1], [0 1 0] or [1 0 0] is changed at random within a range of 0.1 nm. The relative probability of acceptance is:

$$\frac{P_{new}}{P_{old}} = \exp\left\{ -\frac{\Delta U - P\,\Delta V - NkT\,\Delta \ln V}{kT} \right\} \quad (4)$$

where V is the volume of the box.

This acceptance test insures a convergence of the pressure to a given value, taken as 0 in this work. It also allows for orthogonal, though non-isotropic, changes in the box shape. This way, the transitions between the cubic $L1_2$ and the tetragonal $L1_0$ phases are possible. The achievement of the thermodynamic equilibrium is judged by controlling the evolution of instantaneous quantities as cohesive energy, partial concentrations of atomic species, and pressure. Typically, two to six millions macro MC steps are used in order to reach local equilibrium at the atomic scale in both bulk materials and in nanoclusters. Given the larger number of factors and screening effects in the MEAM, the CPU time required for computing the configuration energy is more than five times larger than with the EAM. Therefore, some

MEAM calculations are not carried on with the same statistics as EAM ones.

2.3. Order parameters

One of the aims of the current work is to find out whether the clusters at equilibrium have an ordered structure or not. for this purpose, we need order parameters for the CoPt $L1_0$ and Co_3Pt $L1_2$ structures. In the $L1_0$ structure, each atom has four nearest neighbours of the same atom type and eight nearest neighbours of the other atom type. In the disordered state, all the atoms have equal number of neighbours of both kinds. On this basis, we can define the order parameter of CoPt for each atom as follows:

$$\eta_{L1_0} = 6(\gamma^{A}(B) - 0.5) \quad (5)$$

where $\gamma^{A}(B)$ is the fraction of A—first neighbours of atom B. The parameter is equal to 0 for the disordered state and it is equal to 1 for the ordered state. In order to get the order parameter for the whole sample it is necessary to average this value over all atoms. For clusters, we perform this average only over atoms having exactly 12 nearest neighbours. Surfaces are excluded from the analysis.

In the $L1_2$ structure, each B atom has 12 A nearest neighbours, which is the case for Co_3Pt. In the disordered state, the fraction of Co atoms around each Pt atom is equal to 0.75. So, we can define the order parameter of Co_3Pt around each Pt atom as follows:

$$\eta_{L1_2} = 4(\gamma^{B}(A) - 0.75) \quad (6)$$

where A stands for Pt and B for Co.

To get the order parameter for the whole sample, the parameter is again averaged over all Pt atoms. Eqs. (5) and (6) are valid for measuring order in stoichiometric systems.

3. Results and discussion

3.1. Bulk properties

The CoPt system is well documented in the literature and experimental phase diagrams are now well known for a large-range of compositions [19]. They are characterised by a fcc solid solution at temperatures above 1100 K and several structural phases at low temperature with long-range order. Sweeping in compositions from pure Pt to pure Co, the sequence of equilibrium phases is fcc, $L1_2$, $L1_0$, $L1_2$, hcp, corresponding to Pt_xCo_{1-x} compositions with $x = 1$, 0.25, 0.5, 0.75, 1, respectively. The $L1_2$ phases are of $AuCu_3$ and Au_3Cu type. They are formed by four cubic sublattices of which three are occupied by identical species. The $L1_0$ phase is ordered tetragonal with a breakdown of the cubic symmetry subsequent to the alternate stacking of pure Co and pure Pt{1 0 0} planes. The transition between the ordered phases and the solid solution is first order and is thus characterised by well-defined transition temperatures measured experimentally in [19] for the CoPt and the $CoPt_3$ systems, the case of the Co_3Pt system being less documented.

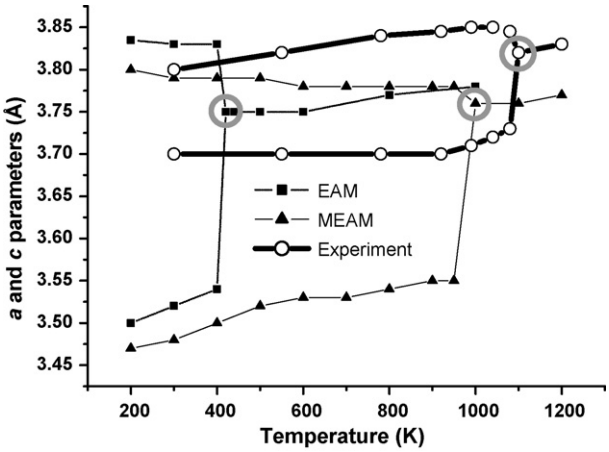

Fig. 1. Lattice a and c parameters of bulk CoPt as functions of temperature. The results obtained with the EAM, the MEAM and experimentally are compared. In each case where a and c are different, the c parameter has the lowest value. The grey open circles indicate the points at which the structural $L1_0$-fcc phase transition occurs. The highest (1100 K) is the experimental transition temperature and the lowest (400 K) is obtained with the EAM potential. The transition temperature predicted with the MEAM is 1000 K.

Nevertheless, the available experimental data already allow substantial assessment of cohesion models, and here we put particular emphasis on the $L1_0$ phase. Its structure is characterised by an alternate sequence of pure Co and Pt{1 0 0} planes whose equidistance, noted as c in what follows, is smaller than that measured in the two other directions, noted as a in what follows. This asymmetry is characterised by a c/a ratio, which is temperature dependent and is unity above the transition temperature.

In Fig. 1, the parameters a and c are represented as functions of temperature and the values obtained with the EAM and the MEAM potentials are compared with experiment. The MC sampling is achieved in the canonical (NPT) ensemble applied to a simulation box containing 864 atoms. A first order transition is clearly observed in the three sets of results, allowing the determination of the order–disorder transition. There is an excellent quantitative agreement between the MEAM model ($T_{OD} = 1000$ K) and experiment ($T_{OD} = 1100$ K). The transition temperature predicted by the EAM model is $T_{OD} = 400$ K. At lower temperatures, the parameter is reasonably well predicted by both models. Its temperature dependence, however, is not seen in the model results. The EAM value (0.383 nm) is a little higher than the MEAM one (0.378 nm) and fits better in the average experimental value (0.382 nm). The predicted c parameters are both lower than experimental (0.37 nm) showing that the predicted asymmetry is too large, in particular, as the MEAM is concerned. It is predicted to increase with temperature, which is not found experimentally. Consequently, the thermal evolution of the c/a ratio in the ordered phase is predicted by both models opposite to the experimental prediction. Above the transition temperature, there is some indication of a predicted and an experimental positive thermal expansion coefficient. Results, however, are too sparse to be conclusive on this point.

We now investigate the extent to which the stable phases are predicted by the models. To this purpose, the MC sampling is performed in the semi-grand-canonical ensemble ($\Delta\mu$-NPT)

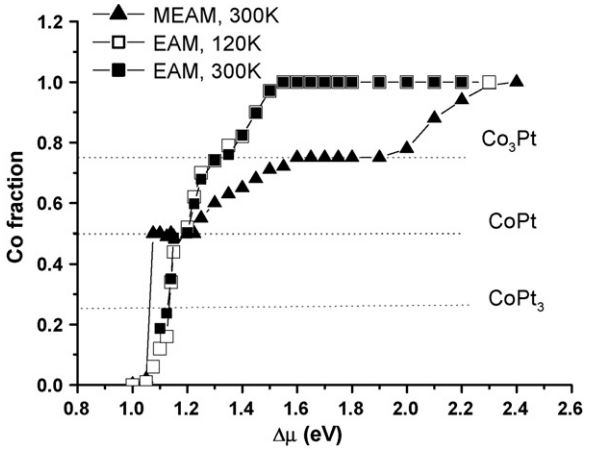

Fig. 2. Dependency of the Co fraction on the chemical potential difference obtained with the EAM and the MEAM. The MEAM isotherm is 300 K, which represents $0.27T_{OD}$. The EAM predictions are shown at $0.27T_{OD}$ (120 K) and at 300 K. The two EAM isotherms cannot be distinguished. Both potentials predict the correct CoPt and Co_3Pt phases. The $CoPt_3$ ordered phase is predicted by none of the potential.

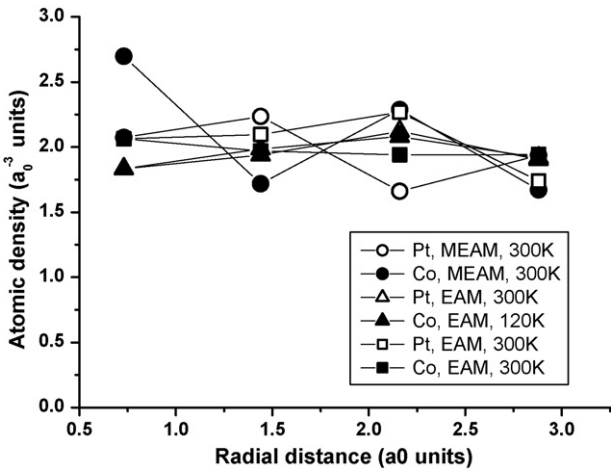

Fig. 3. Radial distributions of the atomic densities of Co and Pt in the CoPt cluster. The MEAM results are given at 300 K and the EAM at 300 K and 120 K. No evidence of segregation is found.

in which, thanks to transmutation trials, the composition freely evolves and the equilibrium composition is governed by the fixed chemical potential difference between the Co and the Pt subsystems. Equilibrium compositions are given for both models as functions of $\Delta\mu$ in Fig. 2. For the purpose of comparison, the temperature is taken as $T = 0.273T_{OD}$, which corresponds to 120 K for the EAM and 300 K for the MEAM. The EAM results at $T = 300\,K = 0.75T_{OD}$ are shown too. Both models predict two ordered phases characterised by Eqs. (5) and (6), corresponding to the plateaus observed in Fig. 2 for the MEAM. One is the CoPt $L1_0$ phase and the second is the $CoPt_3$ $L1_2$ ordered phase.

No semi-empirical potential is perfect and they are tributary of the assumptions made in their construction. The above comparison shows that, qualitatively, with the noticeable exception of the temperature dependence of the *c/a* ratio, most properties of the known experimental phase diagram are reproduced. The predicted values of the *c* and *a* parameters are quantitatively well satisfactory, as they match the experimental measurement within 5% in the worthiest case. The order–disorder transition predicted by the MEAM closely matches the experimental value and confirms the former estimate in [6].

The above comparison shows that it is not possible to make a clear cut decision about which model potential is the best matching experiment since it depends on which property is concerned. For this reason, the study of nanoclusters is performed with both.

3.2. Nanoclusters properties

No assumption is here made about the cluster morphologies. They are built by cutting a spherical arc in a bulk material and letting them evolve toward equilibrium by using the MMC algorithm described in Section 2. The cluster sizes are selected as representative of experimental conditions [4,5]. A CoPt clusters containing 532 atoms is modelled at 300 K and, in the case of the EAM potential, at 120 K as well. In this modelling, no transmutation is attempted and the number of particles of each species is constant. As a consequence, segregation, if any, is necessarily accompanied by a decrease of the order in the cluster core. Fig. 3 shows the radial density distributions obtained. Since the cluster radius is no more than 2.75 lattice units, a detailed radial distribution is not possible. The cluster was subdivided into four concentric layers of equal thickness and Pt and Co densities were evaluated in each layer as an average over several hundreds of configurations sampled over 10^6 MMC macrosteps. There is no atom at the cluster centre, which is an octahedral site. In this case, for an ordered $L1_0$ structure, equal layer thickness distribution results in a constant concentration radial distribution. Accounting for this, the results in Fig. 3 are sufficient to demonstrate that none of the model predicts significant segregation at the CoPt cluster surface and, with the EAM, this result is not sensitive on temperature. The values of the order parameters η is found above 0.8 at $T = 0.27T_{OD}$ with both models. Increasing the temperature to $0.75T_{OD}$ with the EAM model only induces a limited degradation of structural order ($\eta = 0.7$ at 300 K). This partial order was not detected experimentally [5] and the reason for this difference still needs to be elucidated.

The situation is trickier as the Co_3Pt cluster is concerned. The model cluster contains 500 atoms. Using similar layers as for analysing the CoPt cluster, the ratio of the number of Pt and Co atoms is estimated as a function of the distance from the cluster centre. The results with both potentials are displayed in Fig. 4. Because of the apparent high fluctuations, calculations were performed with improved statistics. EAM results were obtained by computing averages over several thousand configurations sampled within 6×10^6 MMC macrosteps. The MEAM results at 300 K were obtained, after equilibration over 10^6 steps, by sampling one hundred configurations over 2×10^6 macrosteps and the calculation was repeated with sampling 2000 configurations over 4×10^6 further macrosteps. Both results are given, indicating that the structure of the radial distributions found are of no statistical fluctuations. At 120 K and 300 K, the EAM predicts a stoichiometric surface layer, and thus no segre-

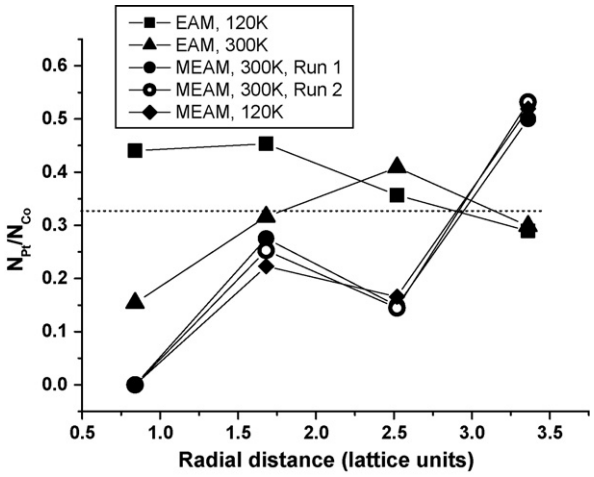

Fig. 4. Radial distribution of the ratio of the number of Pt atoms, N_{Pt}, and the number of Co atoms, N_{Co} in the Co_3Pt cluster. MEAM and EAM results are given at 300 K and 120 K. The MEAM simulation was repeated with two stochastically independent samples, one of 100 configurations over 2×10^6 MC macrosteps (Run 1) and another with 2000 configurations over 4×10^6 macrosteps (Run 2). Both predict an oscillation in the radial distribution leading to an equal fraction of Co and Pt in the outer layer.

gation. The MEAM predicts a composition oscillation leading to such efficient Pt segregation that the surface stoichiometry becomes CoPt. The EAM results at 300 K show a similar, though weaker, trend in the same direction. This enrichment occurs at the expense of the Pt concentration in the core. The MEAM predicts no Pt at all at the cluster centre. The same results are found at low temperature. Further calculations are in progress in order to elucidate ordering in this cluster, which represents a case where experiment may play a decisive role in the assessment of the model.

4. Conclusion

This work demonstrates the sensitivity of the properties of Co–Pt systems on the model potential, one being isotropic and the second allowing for angular dependency in binding energies. The order–disorder transition temperature is much better predicted by the MEAM potential while the *c* and *a* parameters in CoPt are better predicted by the EAM potential. The predicted *c* parameter is lower than the experimental one with both. Both predict the correct CoPt and Co_3Pt ordered structure. The dependence of the relative concentrations on the chemical potentials difference between the two subsystems suggests that the MEAM potential predicts better phase stability.

Given the imperfectness of both potentials for bulk predictions, both were used for cluster predictions and compared. Both predict partially ordered $L1_0$ phase for CoPt clusters and the lack of segregation. Platinum segregation is predicted by the MEAM in the Co_3Pt cluster and none by the EAM potential. The segregation of Pt leads to an equal surface concentration of both species and a pure Co cluster centre. The effect is large enough to hope that experimental measurements might discriminate between the two potentials employed.

Acknowledgements

The authors are thankful to L. Favre and V. Dupuis for stimulating discussions. This work is achieved in the frame of the Belgian network IAP 5-1 “Quantum Size Effect in Nanostructured Materials”. One of us (P.M.) acknowledges a research grant of the Belgian National Science Foundation under contract F.R.F.C. 2.4520.03F.

References

[1] T.G. Dietz, M.A. Duncan, D.E. Powers, R.E. Smalley, J. Chem. Phys. 74 (1981) 6511.
[2] B. Prével, L. Bardotti, S. Fanget, A. Hannour, P. Mélinon, A. Perez, J. Gierak, G. Faini, E. Bourhis, D. Mailly, Appl. Surf. Sci. 226 (2004) 173.
[3] J. Bansmann, S.H. Baker, C. Binns, J.A. Blackman, J.-P. Bucher, J. Dorantes-Da’vila, V. Dupuis, L. Favre, D. Kechrakos, A. Kleibert, K.-H. Meiwes-Broer, G.M. Pastor, A. Perez, O. Toulemonde, K.N. Trohidou, J. Tuaillon, Y. Xie, Surf. Sci. Rep. 56 (2005) 189.
[4] L. Favre, S. Stanescu, V. Dupuis, E. Bernstein, T. Epicier, P. Mélinon, A. Prerez, Appl. Surf. Sci. 226 (2004) 265.
[5] V. Dupuis, L. Favre, S. Stanescu, J. Tuaillon-Combes, E. Bernstein, A. Perez, J. Phys. C 16 (2004) S2231.
[6] S.I. Park, B.-J. Lee, H.M. Lee, Scripta Mater. 45 (2001) 495.
[7] R.A. Johnson, Phys. Rev. B 39 (17) (1989) 12554.
[8] R.A. Johnson, Phys. Rev. B 41 (14) (1990) 9717.
[9] M.I. Baskes, Phys. Rev. B 46 (5) (1992) 2727.
[10] M.I. Baskes, R.A. Jonson, Modell. Simul. Mater. Sci. Eng. 2 (1994) 147.
[11] G. Wang, M.A. Van Hove, P.N. Ross, M.I. Baskes, J. Chem. Phys. 121 (11) (2004) 5410.
[12] M. Hou, M. El Azzaoui, H. Pattyn, J. Verheyden, G. Koops, G. Zhang, Phys. Rev. B 62 (2000) 5117 [10b].
[13] T. Van Hoof, M. Hou, Eur. Phys. J. D29 (33) (2004) 33.
[14] A. Dzhurakhalov, A. Rasulov, T. Van Hoof, M. Hou, Eur. Phys. J. D31 (2004) 53.
[15] M.I. Baskes, Mater. Chem. Phys. 50 (1997) 152.
[16] H. Rose, J.R. Smith, F. Guinea, J. Ferrante, Phys. Rev. B 29 (1984) 2963.
[17] M.P. Allen, D. Tildesley, Computer Simulation of Liquids, Clarendon Press, Oxford, 1987.
[18] S.M. Foiles, Phys. Rev. B 32 (1985) 7685.
[19] C. Leroux, M.C. Cadeville, V. Pierron-Bohnes, G. Inden, F. Hinz, J. Phys. F 18 (1988) 2033.